Development and Validation of a Load Moment Predictive Model for the Prevention of Low Back Pain and Functional Disability

Final Report

for the

Marshall Plan Foundation

6. Juli 2019

by

Alexander Wiesinger

Supervisors:

Prof. Carisa Harris Adamson, PhD

FH-Prof. PD Dr. Thomas Haslwanter

Eidesstattliche Erklärung

Ich erkläre eidesstattlich, dass ich die vorliegende Arbeit selbstständig und ohne fremde Hilfe verfasst, andere als die angegebenen Quellen nicht benutzt und die den benutzten Quellen entnommenen Stellen als solche gekennzeichnet habe. Die Arbeit wurde bisher in gleicher oder ähnlicher Form keiner anderen Prüfungsbehörde vorgelegt.

Linz, am 22. Juni 2019

Alexander Wiesinger

Declaration

I hereby declare and confirm that this thesis is entirely the result of my own original work. Where other sources of information have been used, they have been indicated as such and properly acknowledged. I further declare that this or similar work has not been submitted for credit elsewhere.

Linz, June 22th 2019

Alexander Wiesinger

Acknowledgements

I want to thank Prof. Carisa Harris-Adamson from the University of California, Berkeley, who made my research stay in Berkeley possible in the first place. I truly do not take it for granted to have the possibility to conduct research at one of the best universities in the world. She allowed me to get valuable insight into the professional execution of research studies and all the opportunities as well as problems that arise in the world of academia. Furthermore, she made me feel welcome the second I arrived in the US and supported me in every aspect, whether it was of professional or private nature.

I also want to thank all of my colleagues at the UC Ergonomics Research & Graduate Training Program who accepted and supported me from the first day I have arrived here. I am proud to say that we got to know each other as colleagues and said goodbye to each other as friends. I want to especially mention Elias Höglinger here, as he introduced me to my project and showed me the way around Berkeley when I first arrived here. Venkat Venkatasubramanian and his company Swiftmotion Inc. shall also be mentioned here. He allowed me to work on the SpineTrack project and gave me important insight, especially in the commercial aspects of research.

I am very grateful to Prof. Drew Smith and Dr. Stephen Hill from the Motion Analysis Research Center at the Samuel Merritt University in Oakland. They allowed me to use their high-tech equipment for the purpose of my project and supported me during the execution of the validation study.

I want to thank my supervisor Prof. Thomas Haslwanter as he also made my research stay possible, by giving me valuable input on the application process. Furthermore, he always helped me out when questions, regarding the thesis or the research in general, arised from my side.

Last but not least, I want to thank my family and friends who supported me during my whole research stay. They cheered me up when I needed it the most and I am very grateful for that.

Kurzfassung

Krankenstand, der durch arbeitsbedingte Muskel-Skelett-Erkrankungen (MSEs) hervorgerufen wird, kostet US-Arbeitgebern 60 Milliarden Dollar jährlich. Die häufigste Ursache dieser MSEs ist Überanstrengung im Beruf, weshalb ein besonderer Fokus auf die Verminderung dieser Ursache gelegt werden sollte. Aus diesem Grund hat das UC Ergonomics Research & Graduate Training Program ein leichtes (<0.7 kg), tragbares System entwickelt mit dem es möglich ist die Kinematik des menschlichen Körpers aufzunehmen und zudem ausgeführte körperliche Aktivitäten zu erkennen. Dazu werden "inertial measurement units" in Kombination mit einem künstlichen neuronalen Netz verwendet. Trägt ein Arbeitnehmer das System nun über einen ganzen Arbeitstag, ist es möglich die körperlichen Anforderungen seines Berufes zusammenzufassen. Dies könnte unser heutiges Wissen über den Zusammenhang zwischen körperlichen Anforderungen und dem Auftreten von MSEs bereichern. Die Vorhersagen des neuronalen Netzes bezüglich der ausgeführten körperliche Aktivitäten wurden dann mit den tatsächlichen ausgeführten Aktivitäten mithilfe von Videoanalyse verglichen. Die Aktivitäten wurden mit einer Präzision von 96.66% (4765 Vorhersagen) richtig erkannt. Zusätzlich wurde die Kombination des beschriebenen Systems mit weiteren Technologien, die es ermöglichen die Kräfte die während der körperlichen Aktivitäten auftreten, bewertet. Das beschriebene System stellt eine neue Möglichkeit dar, körperlichen Anforderungen von Berufen zusammenzufassen, da es direkt am Arbeitsplatz verwendet werden kann.

Abstract

The annual costs of workers compensation caused by work-related musculoskeletal disorders (WMSDs) accumulate up to $60 billion in the US. As overexertion is the main contributor to these WMSDs, one approach to decrease the costs is to develop a device which can track physical activities related to overexertion. Workers shall then be equipped with the device across their work-day which summarizes the physical demands of their jobs. This would improve our understanding of the relationship between physical demands and the occurrence of WMSDs. In response to this need, the UC Ergonomics Research & Graduate Training Program has developed a light (<1.5 lbs), low-cost wearable device called SpineTrack which quantifies the kinematics of the trunk and the extremities using inertial measurement units (IMUs). A deep learning model was implemented which allows the prediction of different physical activities by using the data generated by the IMUs. The predictions were compared to the gold standard approach of video analysis. An overall accuracy of 96.66% (4765 guesses) was achieved for predicting correct movements. Additionally the possibility of acquiring the load moment which is acting on the low back during physical activities was explored, as the low back load moment is a main contributor to the occurrence of WMSDs. Therefore, the suitability of combining other wearable technology, which allows the tracking of the ground reaction forces and SpineTrack was investigated. SpineTrack can be seen as a novel approach for summarizing physical demands of jobs, as it can be used directly on the job-site.

Executive Summary

In the United States, the physical demands of a job must be quantified for use in the employment process. When jobs are posted, the physical demands of the job are provided to applicants. Additionally, when an injury occurs, the physical demands of a job are referred to during the return to work process to ensure that workers regain the physical capacity required to perform their jobs. However, currently, the physical demands of a job are primarily quantified using observational techniques which lack accuracy and reliability. Thus, improved quantification methods are warranted and can be further used to improve our understanding of the relationship between job demand and work related musculoskeletal disorders (WMSDs), a problem that costs the US nearly $60 billion per year in the form of workers compensation costs (Liberty Mutual Insurance, 2018). In response to this need, the UC Ergonomics Research & Graduate Training Program has developed a light (<1.5 lbs), low cost wearable device called SpineTrack which quantifies the kinematics of the trunk and the upper extremities using inertial measurement units (IMUs) and predicts common physical activities summarized in a physical demand job analysis. The purpose of this thesis was to first optimize and then quantify the accuracy of the device when compared to the gold standard approach of video analysis. Additional goals were the validation of the generated kinematics, as well as exploring the possibility to acquire the load moment acting on the low back during physical activities.

A laboratory validation study was performed on a sample of convenience. Potential subjects were included in the study if they were between the ages of 18-65, were familiar with tools used in manual materials handling (MMH) jobs and had no chronic disorders (i.e. back pain). This study was approved by the University of California at Berkeley. First, a series of activities (i.e. lifting/lowering, carrying, etc.) were performed sequentially for a set duration or frequency. Next, subjects performed occupational tasks that included a variety of physical activities typically performed in MMH-jobs (i.e. drilling, painting). Tasks were video-taped and analyzed at 30 frames per second. The predicted activity using IMU data was compared to the actual activity from video analysis. Seventy percent of the generated IMU data collected was used to train a deep learning model (training data) to predict physical activities of the other 30% of the data (test data), producing a confusion matrix for each person that summarized the percentage of time each activity was correctly predicted versus incorrectly identified as another activity. The kinematics of SpineTrack were validated using a nine camera motion capture system and the corresponding computed joint angles from the two systems were compared to each other. The ground reaction force during physical activities was acquired using force plates as well as pressure sensing insoles. The force output of the two systems were then compared to each other in order to assess the suitability for the computation of the load moment acting on the low back.

The laboratory validation study consisted of 17 healthy subjects (10 males) with an average age of 31 ± 13.6 years. The average height and weight of individuals were 169.4 ± 14.8 cm and 68.2 ± 15.6 kg, respectively. For predicting correct activities in the test data an overall accuracy of 96.66% was achieved. Walking was correctly classified 90.06% of the time and was mostly mistaken with crouching (1.6%) and

crawling (3.2%). Static overhead activity was correctly classified 94.76% of the time and was mostly mistaken with dynamic overhead activity (4.0%). Reaching for a nearby object was correctly classified 93.15% of the time and was mostly mistaken with dynamic overhead activity (1.6%), reaching for an object on shoulder height (0.9%), crawling (1.8%) and crouching (1.8%). Qualitatively speaking, the kinematics generated by SpineTrack show a high correlation to the motion capture data. However, the acquired force data using pressure sensing insoles was unreliable and at the time of writing, the force data provided by the force plates was used to estimate the load moment acting on the spine.

The results of the small pilot validation study regarding the activity prediction process showed a high overall accuracy. However, the model still confuses dynamic activities which are similar to each other. Despite the benefits of identifying the percent time spent performing different physical activities, the magnitude of loads handled and load moments are not yet fully implemented in this technology. Further work should include additional advancements that can be used to quantify load and/or load moment. The opportunity to classify physical demands in different job sectors using objective methods such as IMUs will allow better quantification of the physical requirements of a job that can be used for effective surveillance and return to work programs.

Contents

1 Introduction **11**
- 1.1 Work-related musculoskeletal disorders . . . 11
  - 1.1.1 Causes and risks . . . 11
  - 1.1.2 Prevention . . . 13
  - 1.1.3 Low back pain . . . 14
  - 1.1.4 Physical demands of jobs . . . 15
- 1.2 Problem statement . . . 15
- 1.3 Goals and non-goals . . . 16
- 1.4 Structure of the thesis . . . 16

2 Material and Methods **17**
- 2.1 SpineTrack . . . 17
  - 2.1.1 Inertial measurement units . . . 17
  - 2.1.2 Data transmission . . . 20
- 2.2 Activity prediction . . . 21
  - 2.2.1 Data acquisition . . . 21
  - 2.2.2 Data Post-processing . . . 22
  - 2.2.3 Computation of joint angles . . . 23
  - 2.2.4 Deep learning model . . . 25
- 2.3 Additional features . . . 26
  - 2.3.1 Load moment estimation . . . 26

3 Results **31**
- 3.1 Kinematics . . . 31
- 3.2 Activity prediction . . . 32
- 3.3 Load moment . . . 33

4 Discussion and Outlook **38**
- 4.1 Kinematics . . . 38
- 4.2 Activity prediction . . . 39
- 4.3 Load moment . . . 40
- 4.4 Conclusion and outlook . . . 41

List of Figures

1.1 Applied load and structure tolerance of the spine 12
1.2 Determination of WMSD Risk 13

2.1 Global and body-fixed reference frames 18
2.2 Computation of IMU orientation and position 19
2.3 Segmentation of the recorded activities 23
2.4 Defined joint angles 24
2.5 Training split of the deep learning model 26
2.6 Determination of the spinal load moment 27
2.7 Definition of the horizontal distance h 28
2.8 Pressure sensing insoles 29

3.1 Computed spine angle 32
3.2 Computed shoulder flexion angle 33
3.3 Computed elbow flexion angle 34
3.4 Computed thigh inclination angle 35
3.5 Recording of physical activities using SpineTrack 35
3.6 Recording of a physical activity using SpineTrack, a motion capture system, force plates and pressure sensing insoles 36
3.7 Kinematic and kinetic analysis of the hip flexion angle 36
3.8 Comparison of force plates and pressure sensing insoles 37

List of Tables

2.1 Defined physical activities 22
2.2 Anthropometric data 29

List of Abbreviations

ADA	Americans with disabilities act
CTS	Carpal tunnel syndrome
DALY	Disability adjusted life years
GUI	Graphical user interface
IMU	Inertial measurement unit
IRB	Institutional review board
LBD	Low back disorder
LBP	Low back pain
LSTM	Long short-term memory
MARC	Motion Analysis Research Center
MMH	Manual materials handling
MSE	Muskel-Skelett-Erkrankungen
REBA	Rapid entire body assessment
RULA	Rapid upper limb assessment
SHARP	Safety and health assessment and research for prevention
WMSD	Work-related musculoskeletal disorder

1 Introduction

The purpose of this thesis is to continue the development of a device which allows the tracking of physical activities performed by workers across a work-day. This device is aimed to be used in the manual materials handling (MMH) job sector and ultimately its purpose is to give an overview on the risk of developing work-related musculoskeletal disorders (WMSDs) for different jobs. The following chapter shall give an introduction and provide a general overview on the current problems in today's occupational environments.

1.1 Work-related musculoskeletal disorders

This section aims to give an overview on WMSDs, their causes and which tools can be used to minimize their occurrence. Furthermore, facts on low back pain are presented as it is the number one cause for WMSDs. At the end of the section, the current method of determining physical demands of jobs is detailed.

WMSDs are defined as a relative diverse group of painful disorders that arise in occupational environments. However they all have in common that they affect parts of the human body which are associated with movement. This means that all joints, muscles, ligaments, tendons etc. can be affected by WMSDs. Simoneau et al. (1996) summarized that WMSDs can arise from overuse and gradual development, that they can be prevented very effectively and that they can also have multiple causes. Typical examples of WMSDs are Carpal Tunnel Syndrome (CTS), Tension Neck Syndrome, Low Back Disorders (LBDs) and different forms of tendinitis [2, 26].

In 2018, these WMSDs accounted for around $60 billion in workers compensation costs in the United States. 23.4% of these costs were related to overexertion, which is caused by physical activities like gripping, pushing/pulling, lifting, carrying and holding, making overexertion the single biggest contributor to WMSDs. The rest of these costs is split up between falls, slips and other accidents [14].

1.1.1 Causes and risks

The activities related to overexertion are often performed in a forceful manner and without adequate recovery time which can lead to musculoskeletal fatigue and subsequently injury over time [2]. McGill (1997) defined the occurrence of injuries in this aspect as "when the applied load exceeds the failure tolerance or strength of the tissue" [18]. Fig. 1.1 displays two cases in which injury can occur, (a) being a traumatic- and (b) being a chronic spine injury.

Fig. 1.1(b) can be seen as especially relevant for WMSDs as overexertion caused by repetition is displayed in this figure. An example of this repeating loading pattern,

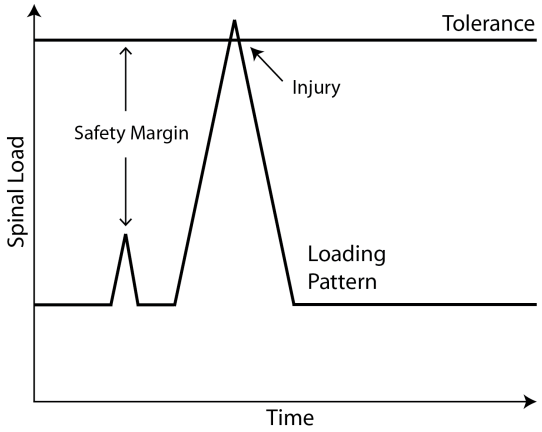

(a) The loading pattern starts well below the structure tolerance of the spine. Due to a very fast change of spinal load, (e.g. car accident) a traumatic injury occurs as the structure tolerance of the spine is surpassed. Figure adapted from Fig. 1 in [18].

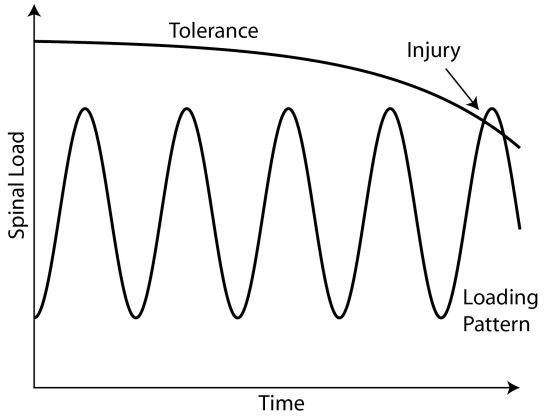

(b) The loading pattern starts within the structure tolerance of the spine. As a whole work day passes by, the structure tolerance decreases as a result of spinal tissue fatigue. This can lead to cumulative trauma and injury as the margin of safety becomes zero over time. Figure adapted from Fig. 3(c) in [15].

Figure 1.1: Relationship between applied load and structure tolerance of the spine. Depending on the amount of time spent in repetitive work, the structure tolerance of the spine decreases due to fatigue, while the injury risk increases. Additionally, particularly fast changes in spinal load can lead to an injury without the need of any preexisting fatigue.

which can cause a chronic injury could be the lifting of boxes in a warehouse across a whole workday. The repeated movement leads to overexertion and fatigue of the spinal tissue. This overexertion explains the occurrence of occupational injuries while performing seemingly easy tasks. Duration and frequency of the task, next to repetition, complete the three major modulators which contribute to WMSDs. The higher these three modulators are, the greater the risk of the occurrence of WMSDs is [26].

Additionally to these major modulators, Simoneau et al. (1996) defined and described the following risk factors which furthermore contribute to the occurrence of WMSDs [26]:

- Awkward posture: Maintaining joints near the limit of their range of motion, maintaining body segments with a disadvantage relative to gravity or holding positions which restrict the blood flow can lead to fatigue.
- Musculoskeletal load: This factor depends on the involved joint, the maintained posture, the required force, the grip used, as well as the direction of effort. If the required forces for a task surpass the capability of the worker, injury risk increases.
- Static work: Static work (e.g. overhead work) can lead to an under-supply of blood in the muscles, leading to fatigue.

- Exposure to physical aggressors: Mechanical pressures, shocks/impacts and prolonged exposure to vibrations have been linked to the occurrence of WMSDs [6].
- Invariability of work: This factor is closely linked to the repetition-modulator and a causal relationship to the occurrence of CTS has been found in previous research [21].
- Organizational factors: Work load, work pace as well as social environment can heavily influence fatigue.

Fig. 1.2 displays the combination of the modulators and risk factors leading to the overall risk of the occurrence of WMSDs.

Figure 1.2: The combination of the three major modulators repetition, duration and intensity with additional risk factors (e.g. awkward posture, musculoskeletal load, etc.) describes the risk of the occurrence of WMSDs. Figure adapted from Fig. 2.1 in [26].

1.1.2 Prevention

In order to get an overview on how WMSDs can be prevented, a few definitions have to be made first.

Manual materials handling is defined as "moving or handling things by lifting, lowering, pushing, pulling, carrying, holding, or restraining" [2]. A causal relationship between often performed activities in MMH, like heavy physical work, lifting, forceful movement and the occurrence of low back pain (LBP) has been found in previous research [21, 27].

Ergonomics is the design of processes and machines, the layout of workplaces, the methods of work and the control of the physical environment when considering the humans who work with these machines in the specified conditions [25]. It is basically fitting the workplace to the worker and it aims to prevent WMSDs by applying different principles to identify, evaluate and control the risk factors previously mentioned, in different occupational environments [27].

A variety of such principles and tools exist, the most important ones shall be briefly mentioned here:

- Revised NIOSH Lifting Equation [30]: This equation can be used to identify hazardous lifting tasks. It can decrease the occurrence of WMSDs by making suggestions on how to optimize lifting (e.g. change origin/destination-heights). It furthermore specifies what the recommended weight limit for a given lift is.

- Rapid Upper Limb Assessment (RULA) [17]: This assessment tool can be used to evaluate the risk of WMSDs related to the upper limbs. The joint angles are thereby assessed using classification charts and corresponding risk tables.
- Snook Tables [13]: These tables can be used to analyze lifting/lowering, pushing/pulling and carrying tasks. By entering the lifting height, the handled weight and the frequency of the lift into these tables, the population percentages which are able to execute the lift can be obtained.
- Rapid Entire Body Assessment (REBA) [11]: This tool can be used to analyze and evaluate body postures and allows the computation of the risk for WMSDs regarding different postures. A classification chart similar to the one in RULA is used in this case.
- Hand-Arm Vibration Exposure Calculator [10]: This tool can be used to calculate the exposure to hand-arm vibration and subsequently the risk of developing hand-arm related WMSDs.

These tools are a great source for analyzing hazardous activities at workplaces and have been established in the ergonomics sector for a long time. They have had a significant impact on the reduction of WMSDs in the past.

1.1.3 Low back pain

It is reported that low back pain is the reason for most of the healthcare visits regarding WMSDs in the United States, therefore it shall be discussed in its own section.

In 2012, about 28.8% of the US population (18 years and older) reported having experienced LBP during the last three months. This outweighs other WMSDs by a lot (Knee pain: 18.1%, neck pain 15.2%, upper limbs: 11.2%). Furthermore it is estimated that LBP causes the loss of 818.000 disability adjusted life years (DALY) annually. According to the World Health Organization, one DALY can be thought of as "one lost year of healthy life". Therefore a high focus should be placed on the prevention of this particular disorder [3, 23, 29].

A lot of equations and tools exist in order to compute the risk of injury regarding the low back. However most of them simplify the specific anatomical structure of the low back and focus on computing the general biomechanical demand on the spine. McGill (1997) summarized specific approaches to analyze individual tissue injury, which certainly is the most accurate way of determining LBP-risk [18]. However, such an approach would go beyond the scope of this thesis, which is why only one of the most important parameters, the load moment acting on the low back, shall be explained here.

Coenen et al. (2013) found that cumulative low back load, in the form of low back load moments, has the most consistent association with LBP [4]. The single biggest factor which influences the low back load moment during a lifting task is the horizontal distance h between the object being lifted and the low back (specifically the L5S1 joint) of the person. This can be explained by the fact that when h is high, the person is likely to lean forward which means the weight of the trunk multiplied

by the horizontal distance to the center of gravity of the trunk has to be counteracted by a low back moment in order to not fall over. This is the reason why ergonomists generally recommend to bend the knees and keep the object close to oneself while lifting (thus minimizing h), as the reason for injury most of the times is not the lifted object itself, but the low back moment acting on the spine, which is needed to counteract the weight of the trunk.

1.1.4 Physical demands of jobs

The "Americans with Disabilities Act" (ADA) is a civil rights law and was issued in 1990. It prohibits discrimination in all public life areas, including job sectors. In order for disabled people not to be discriminated, it requires employers to state the physical demands necessary to fulfill jobs. Typically these physical demands are obtained using observational techniques, which means that employees, who are performing a job, are monitored by a designated employee across a whole workday and every activity they execute is noted. The following statements are typical examples on how these activities are then summarized in a job description:

- Must be able to stand approximately 50% of the workday.
- Frequently has to move material weighing up to 30lbs across the office.
- Often has to push carts weighing up to 100lbs across the office.

While the ADA is certainly very valuable with regards to anti-discrimination in the job sector, the statements above are not the best solution.

When talking about WMSDs it is crucial that the exact time spent in different physical activities is known, as slight changes in physical activities across a work day could make dramatic differences in the risk of developing WMSDs. Therefore, terms such as "approximately", "frequently" and "often" should be replaced with average time spent in said physical activity. However, when using observational techniques it is quite difficult to exactly determine the amount of time spent in these activities. The observational techniques come with additional problems as the classification of the different activities very much depends on the employee who tracks these activities.

All in all, it can be said that the physical demands of jobs today are not sufficiently classified and need further improvements.

1.2 Problem statement

WMSD related costs account for 23.4% of the overall financial US-national burden [14]. Therefore the Safety and Health Assessment and Research for Prevention (SHARP) Program suggests that WMSDs should be a high priority for injury prevention [24].

One way this could be achieved is by tracking the physical activities related to overexertion that a worker is performing across a whole workday on the job-site and then summarizing the risks associated with these activities. This would provide the

employee with valuable feedback on when to take breaks and also give the employer an overview on the risks of different job tasks. However, up until now, it was not possible to fully classify and summarize the activities and physical demands associated with different jobs. Currently, observational techniques are used to summarize physical demands associated with jobs, which lack accuracy and reliability.

Furthermore, up until now it was not possible to classify low back load moments on the job site which are the number one contributor to WMSDs.

1.3 Goals and non-goals

The purpose of this thesis is to expand a system called SpineTrack, consisting of inertial measurement units (IMUs) which can be used on the job-site, with a deep learning model to predict, quantify and summarize physical activities which occur in MMH jobs. This quantification of activities would allow the computation of the overall risk associated with different jobs. A validation study shall be performed, in order to validate the predictions made by the model. This validation study and the subsequently acquired accuracy-results are the core of this thesis.

The kinematics gathered by the system shall also be validated using golden standard techniques in the form of a motion capture system.

Furthermore, the opportunity of integrating pressure sensing insoles in the SpineTrack system shall be explored, in order to acquire information on the loads handled as well as on the low back load moment.

It is not the goal of this thesis to create a fully developed system which allows the computation of the WMSD-risk. As SpineTrack has been an ongoing project for several years, this thesis shall only give an overview on the current state of the system and the ongoing advancements.

1.4 Structure of the thesis

Chapter 2 describes all the materials and methods used in order to advance the state of the SpineTrack system. It shortly describes all the components implemented in SpineTrack. Next it describes the activity prediction process of the deep learning model, including the data acquisition in the validation study, every aspect on processing the data, the computation of joint angles using the sensor data and the training of the deep learning model. At the end, additional features implemented in SpineTrack are detailed, which allow an estimation of the low back load moment and graphical representations of the computed risk factors from the acquired data.

Chapter 3 first displays results of the validation of the kinematics generated by SpineTrack. These kinematics were validated using a nine camera motion capture system. After that, the results of the activity prediction process are displayed. At the end of this section, results regarding the low back load moment estimation are displayed.

Chapter 4 discusses the gathered results and provides an outlook on future developments of the SpineTrack system.

2 Material and Methods

The following chapter describes all the necessary materials and methods in order to create a device which can quantify and summarize the physical demands of a job. First the device at its current state of development is described. Next, the newly developed activity prediction process is described, including the data generation process and validation techniques. At the end of this chapter, advancements in the estimation of the load moment acting on the spine, using pressure sensing insoles, are described.

2.1 SpineTrack

This section describes the SpineTrack-system, a wearable device which allows to track the orientation of various human body segments over time. The purpose of SpineTrack is to generate data which can be used by a deep learning model in order to predict physical activities. In this section all the components currently implemented in SpineTrack are described.

SpineTrack is a system developed by the UC Ergonomics Research & Graduate Training Program[1] at the University of California, Berkeley, consisting of a wearable vest which contains eight IMUs. The purpose of this system is to track physical activities performed by persons and subsequently allow the computation of the 3D-orientation of body segments during the execution of these physical activities. SpineTrack tracks the orientation of the upper back, lower back, upper arms, lower arms and upper legs. This project is a collaboration between the University of California, Berkeley and SwiftMotion Inc.[2] and is intended for commercial purposes. Therefore, some components implemented in SpineTrack can not be described in detail in this thesis, because of intellectual properties.

2.1.1 Inertial measurement units

Inertial measurement units are sensors which typically include three-axis accelerometers in order to measure linear accelerations, three-axis gyroscopes in order to measure angular velocity and three-axis magnetometers in order to measure the orientation of the local magnetic field. By combining and processing this data it is possible to track the orientation as well as the position of the IMU [9, 32].

In order to define position and orientation, a global reference frame has to be defined first. This global reference frame can be defined as a point in space (e.g. the

[1] `https://www.ergo.berkeley.edu`
[2] `https://www.swiftmotion.io`

initial position of the IMU) with a reference orientation of the sensor being upright (in this case the measured linear acceleration must be zero in two of the three accelerometers and the gravitational acceleration $g = 9.81\,\mathrm{m/s^2}$ in the third one) and aligned to magnetic north and east. Fig. 2.1 displays such a global reference frame (x, y, z) as well as a body-fixed reference frame (x', y', z'). The body-fixed reference frame changes with a change of orientation of the IMU, whereas the global reference frame is defined solely by the starting orientation of the IMU. By applying yaw-, pitch- and roll angle rotations to the body-fixed reference frame, corresponding to rotations around the z'-, y'- and x'-axis, the orientation of the sensor relative to the global reference frame can be determined. This transformation of the body-fixed reference frame back to the original orientation of the global reference frame (x, y, z) is done every time the IMU outputs new raw data from the included sensors, allowing the continuous tracking of its orientation.

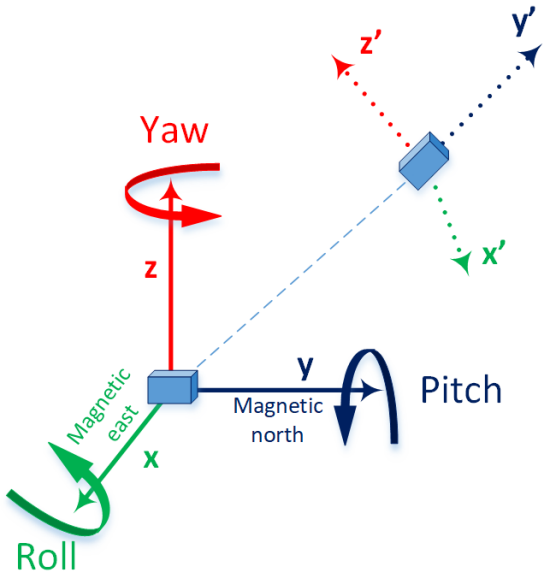

Figure 2.1: The body-fixed reference frame (x',y',z') which tracks the orientation of the IMU (light blue box) can be transformed back to the global reference frame (x,y,z) by applying yaw-, pitch- and roll angles of rotation to it. The position of the IMU is tracked by the positional vector (light blue dashed line).

One must be careful when applying rotations around these axes, as sequences of rotations in 3D-space are non-commutative, meaning the sequence of the rotations matters. Generally speaking, these triple-sequences of single-axis rotations are called Euler-angle representations and include gimbal-lock anomalies [8]. To avoid these anomalies, a more elegant way of rotating in 3D-space is possible, using quaternions. These four-dimensional complex vectors allow one single rotation around a newly computed rotational axis in order to reach the target orientation.

Fig. 2.2 displays the practical algorithm used to compute the orientation as well as the position of the IMU using the provided raw data. When determining the position of an IMU, raw data has to be integrated three times, which means included noise

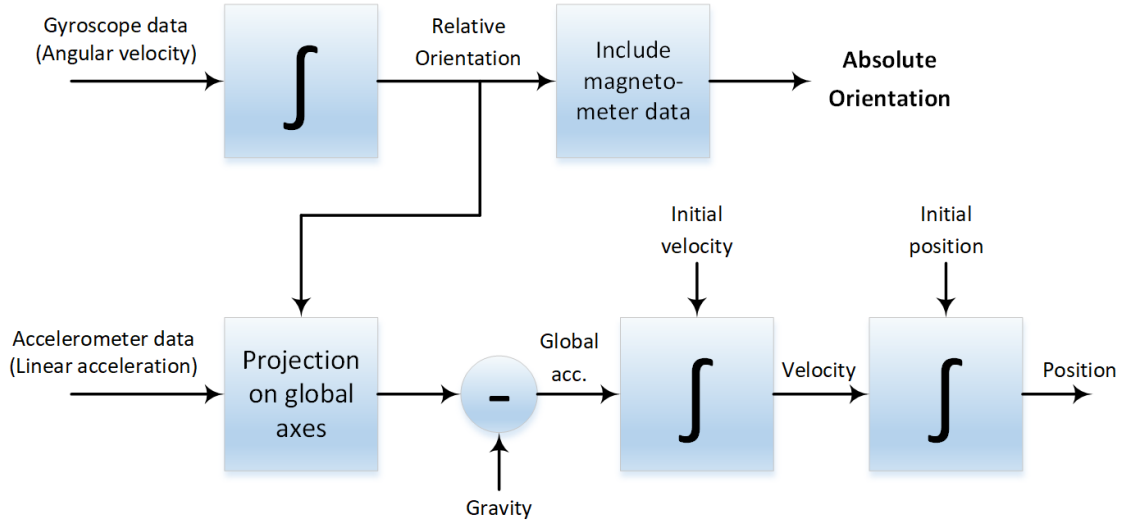

Figure 2.2: Typical algorithm used with IMUs to determine orientation as well as position of the sensor. Integration of the gyroscope data in combination with the magnetometer data allows the computation of the absolute orientation of the IMU. Combining the orientation data with the accelerometer data, subtracting the gravitational acceleration and integrating this resulting data twice with the respective initial conditions allows the determination of the position of the IMU. Figure adapted from Fig 4. in [32].

is also integrated three times. This could lead to significant drifts in the data when tracking the position for a long time. However, in the case of SpineTrack, only the absolute orientation of the IMU is of importance, as solely the orientation of body parts and not their exact location are of interest.

Today a variety of established IMUs exist, from bulky versions used in inertial navigation systems (Oxford Technical Solutions Ltd) to very small ones used in 3D motion tracking (XSens Technologies B.V.). In the case of SpineTrack, it is critical that the sensors are very small, as they should not interfere with any physical activities performed by the person wearing the system. Another critical aspect is the price of the IMUs, which should be as low as possible, as the system is intended to be an affordable solution to quantify and summarize job demands. Considering these arguments, the UC Ergonomics Research & Graduate Training Program has developed its own IMU. The core of the IMU is a board on which a three-axis linear accelerometer, a three-axis gyroscope and a three-axis magnetometer are implemented, making it a nine degrees of freedom system. The raw data collected by the system is directly processed on-board and transformed into a quaternion, as well as Euler angles which determine the current orientation of the IMU with respect to the global reference frame specified by gravity and the local magnetic field (see Fig. 2.1). The sequence of rotation of these Euler-angles which are applied to the body fixed reference frame, is generally defined as ZYZ, meaning the first rotation occurs around the z-axis, followed by a rotation around the y-axis and a rotation around the rotated new z-axis.

The data is filtered using a moving average filter and its long time drift is compensated by the implementation of a high pass filter. Due to reasons of intellectual properties, the exact parameters of the on-board processing and filtering can not be described here.

The anatomical locations of the eight used IMUs in the vest are defined as follows with the sensor ID and abbreviations stated in brackets:

- Between 3rd and 4th thoracic spinous process facing posterior (*0*: *T3T4*)
- Between 5th lumbar and 1st sacral spinous process facing posterior (*1*: *L5S1*)
- Medial part of the left upper arm facing lateral (*2*: *LSH*)
- Medial part of the right upper arm facing lateral (*3*: *RSH*)
- Distal part of the left lower arm facing posterior (*4*: *LWR*)
- Distal part of the right lower arm facing posterior (*5*: *RWR*)
- Medial part of the left thigh facing lateral (*6*: *LTH*)
- Medial part of the right thigh facing lateral (*7*: *RTH*)

With these eight sensors and their corresponding anatomical locations it is possible to track the orientation of the trunk, the upper arms, the lower arms and the upper legs. It shall be mentioned that the exact position of the IMUs is not of major importance, as only the orientation of these sensors is tracked. However, it is important to not place the sensors directly on muscle bellies, as their orientation could then change during the activation of those muscles.

2.1.2 Data transmission

Two WiFi dongles were developed of which each of them can connect to up to four IMUs. By plugging these dongles into USB-ports on a PC, IMU-generated data can be transmitted via WiFi. When the IMUs are switched on they automatically search and connect to the dongles within seconds. The maximum range of transmission is limited to about ten meters, meaning a laptop has to be relatively close to the person wearing the SpineTrack system at all times.

In order to start the recording and receive the data, a MATLAB (Mathworks, Boston, MA, USA) application was created using the MATLAB App Designer, which reads the USB ports that the WiFi dongles are connected to and stores the received data as .csv-files.

Using this application, it was then possible to acquire data which provides information on the orientation of the different body segment. This can be seen as the first step of many, in order to predict which kind of physical activity was performed.

2.2 Activity prediction

The SpineTrack system described in section 2.1 was used in combination with a deep learning model to predict performed physical activities. In this chapter the generation of these activity predictions is described with all its necessary sub-components. This section represents the backbone of the thesis.

A deep learning model was used to predict physical activities performed py persons wearing the SpineTrack system. Therefore the deep learning model had to be trained first to be able to recognize different activities. In order for deep learning models to perform well, a lot of training data is required. Because of this, a study was proposed which aimed to recruit subjects and generate the necessary amount of data.

Using the data provided by the IMUs, human joint angles were then computed for each time step of the recordings. These angles were used as an input for the deep learning model in order for it to predict physical activities.

2.2.1 Data acquisition

The aim of the laboratory validation study described in this section was to generate as much data as possible in order to train the deep learning model sufficiently. Approval by the local Institutional Review Board (IRB) and signed informed consents were obtained before any data acquisition. Subjects were recruited as a sample of convenience, meaning announcements were posted in local social media groups. Chronic conditions (e.g. neck-, back-, arm or vision conditions), unfamiliarity with basic tools used in MMH-jobs (drills, heavy objects) as well as ages below 18 and above 65 were defined as exclusion criteria. Subject specific data was fully anonymized and only referred to using ID-codes.

The study protocol remained the same across all recruited subjects. After the subjects signed the informed consent, body measurements were taken. Specifically lower- and upper leg length, lower- and upper arm length, L5S1 height, neck length, shoulder- and hip width and T3T4 height. Additionally age, height and weight were recorded.

As a next step the different physical activities were performed. Table 2.1 displays all of these activities. These activities were chosen because they represent the most common movements which are executed in MMH-jobs. Generally speaking, all of the 23 activities were repeated 15 times during a recording session and saved as individual .csv-files using the GUI displayed in Fig. **??**. Subjects were instructed to stand still for five seconds between each repetition in order to allow easier separation of the activities during the Post-processing of the data. Subjects were furthermore asked to practice the activities before every recording session and were corrected in case of poorly executed activities. It shall be mentioned that all the lifting-activities consisted of two movements, lifting the weight up and lowering the weight back down. Out of simplicity reasons they are identified using the same ID-number, meaning the deep learning model treats them as the same activity.

Additionally, subjects were asked to perform three occupational tasks (laying carpet, packing bottles, simulating drilling). These tasks were used to analyze the

accuracy of the predictions made by deep learning model when using actual occupational task data.

Table 2.1: Every physical activity performed in the validation study. These activities shall be predicted by the deep learning model. Each activity was assigned to an ID-number.

ID	Activity
0	Carrying with both hands
1	Crawling
2	Crouching
3	Kneeling
4	Lift to 60 cm level
5	Lift to shoulder level
6	Lift to waist level
7	Stooped lift to waist level
8	One handed lift (left) to waist level
9	One handed lift (right) to waist level
10	Lift to shoulder level with axial twist
11	Lift from waist- to shoulder level
12	Dynamic overhead activity
13	Static overhead activity
14	Pulling a cart
15	Pushing a cart
16	Static reaching (close to body)
17	Static reaching (far from body)
18	Static reaching (far and high from body)
19	Sitting
20	Standing
21	Static stoop
22	Walking

Furthermore, subjects were asked to hold static positions with varying elbow-, hip- and shoulder flexion. This was necessary to estimate the previously defined horizontal distance h (see section 1.1.3) using the data generated by the IMUs. The horizontal distance was used to estimate load moment acting on the spine and the process implemented is explained in detail in section 2.3.1.

Subjects were videotaped at 30 frames per second across all performed activities. This video data was then used to validate the predictions made by the deep learning model on the different physical activities.

During and at the end of the trial, subjects completed surveys to rate the usability of the SpineTrack system.

2.2.2 Data Post-processing

Before the IMU-generated data from the physical activities could be used as input for the deep learning model, it first had to be processed. The raw data corresponding to a physical activity stored in .csv-files consisted of multiple repetitions of the physical activity with one continuous time vector. The goal was to create segments of the data which start at time zero for every repetition of the physical activity. Fig. 2.3

displays this segmentation of the data. In order to achieve this segmentation, a MATLAB-script had to be developed.

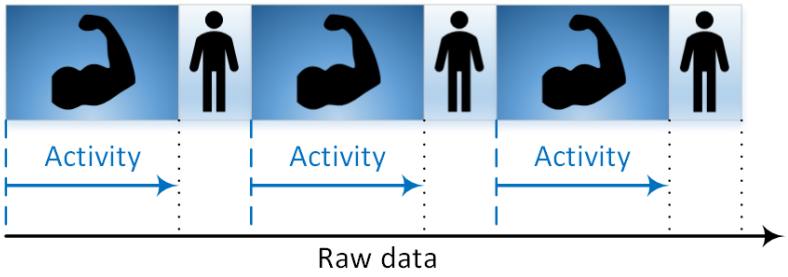

Figure 2.3: The raw data generated by the IMUs and the GUI consists of one specific physical activity followed by the subject standing still. This process repeats another 14 times during one recording session. The goal of the Post-processing of the data is to extract the data of each performed activity, excluding the data where the subject is standing still. These extracted datasets (indicated as blue lines) should have a corresponding time-vector which always starts at $t = 0$.

The processed data could then already be used to train the deep learning model, however as all the sensor data is included, it would accumulate to a huge amount of data with a lot of subjects, slowing down the whole training process. Therefore additional Post-processing was done which combines key sensor-data, generating data of smaller size while at the same time still containing all of the information.

2.2.3 Computation of joint angles

The computation of joint angles was necessary to reduce the amount of data which was used to train the deep learning model. This sped up the training process by magnitudes while preserving the same information content of the original sensor data.

Fig. 2.4 displays the joint angles which were computed using the raw sensor data provided by the IMUs. It shall be mentioned that the hereby displayed angles, represent angles in all three dimensions, commonly described as Euler angles. These angles contain all the necessary information on the current pose a user is performing when combined with the absolute orientation of just one of the IMUs. This would be enough information to create a 3D-model of the person wearing the device, excluding the head and the lower legs/feet. However in the case of SpineTrack, only the joint angles are of interest.

To compute the joint angles, the quaternions streamed by the IMUs were used to calculate a difference quaternion, describing the rotation axis between two IMUs as well as the amount of rotation necessary to transform the orientation of one IMU to the orientation of the other one. This difference quaternion was then transformed to Euler angles, stating the difference in orientation (degrees) using a ZYZ-sequence and allowing meaningful displaying of the joint angle data. Equation (2.1) displays

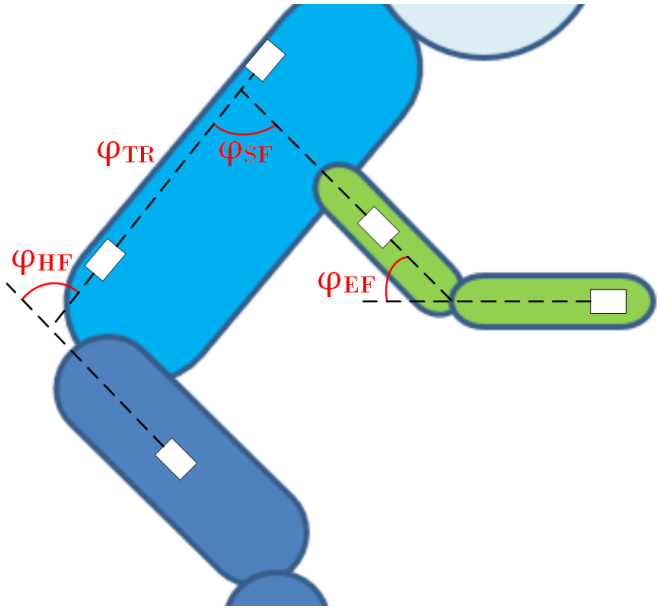

Figure 2.4: Joint angles which were calculated using the IMU-generated data, displayed in red. From the left to right: Hip flexion angle φ_{HF}, trunk angle φ_{TR}, shoulder flexion angle φ_{SF}, elbow flexion angle φ_{EF}. The trunk angle is defined as the difference in orientation between the T3T4-sensor and the L5S1-sensor and is zero in the displayed case for reasons of simplicity.

this computation,

$$\begin{bmatrix} \alpha \\ \beta \\ \gamma \end{bmatrix} = \mathrm{quat2eul}\left({q_1}^{-1} \circ q_2\right) \cdot \frac{180\,^\circ}{\pi} \tag{2.1}$$

where α, β and γ denote the rotation angles around the z-, y- and the rotated new z-axis (rotation sequence: ZYZ) of the relative coordinate frame of one IMU, which are necessary to achieve the same orientation as the second IMU, q_1 and q_2 denote the quaternions streamed from two IMUs, $^{-1}$ denotes an inversion of a quaternion, $\circ$ denotes a quaternion multiplication and quat2eul() denotes a transformation from a quaternion to the corresponding Euler angles.

Eq. (2.2) displays the transformation from a quaternion q to the corresponding Euler angles using the function quat2eul(),

$$\mathrm{quat2eul}(q) = \begin{bmatrix} \arctan\dfrac{2(q_0q_1 + q_2q_3)}{1 - 2(q_1^2 + q_2^2)} \\ \arcsin(2(q_0q_2 - q_3q_1)) \\ \arctan\dfrac{2(q_0q_3 + q_1q_2)}{1 - 2(q_2^2 + q_3^2)} \end{bmatrix} \tag{2.2}$$

where q_0 denotes the scalar part and q_1, q_2, q_3 denote the vector part of the quaternion [1].

This concept of computing the difference quaternion by multiplying one IMU-quaternion with the inverse of a second IMU-quaternion and transforming it to Euler

angles was done in the same way for all of the joint angles. φ_{HF} was determined for the left as well as the right side, using *L5S1* sensor data in combination with *LTH/RTH* sensor data. φ_{TR} was determined using *T3T4*- as well as *L5S1* sensor data. φ_{SF} was once again determined for the left as well as the right side, using *T3T4* sensor data in combination with *LSH/RSH* sensor data. This process was the same for φ_{EF} where *LSH/RSH* sensor data was used in combination with *LWR/RWR* sensor data. These joint angles could then be used in combination with the absolute orientation of one of the IMUs as input for the deep learning model.

The kinematics, generated by SpineTrack, in the form of joint angles were then compared to the golden standard technique of motion capture using a nine camera system (Qualisys AB, Goeteborg Sweden) for validation purposes. Subjects therefore performed functional tasks while wearing the SpineTrack system as well as the markers for the motion capture system. The marker positions can be obtained in Appendix A. The motion capture system recorded at a sample frequency of 100 Hz, directly computed joint angles and stored them in .csv-files which then could be compared to the SpineTrack kinematics. The motion capture data was first downsampled by a factor 10 to match the sample frequency of 10 Hz used by the SpineTrack system before making a comparison.

2.2.4 Deep learning model

The purpose of this deep learning model was to use joint angle data as input and predict which activity was performed in each specific dataset. As the joint angle data represents temporal data, a recurrent neural network, specifically in the form of a long short-term memory (LSTM) neural network was created [12].

Therefore the MATLAB Deep Learning toolbox was used to train and further specify the model. Unfortunately the source code and the model specific settings can not be shared in this thesis as the model was under review for patent-filing at the time of the creation of this thesis.

However, the following can be said about the model. The model uses the in sections 2.2.2 and 2.2.3 defined segmented joint angle data as input and predicts which of the physical activities defined in Table 2.1 was performed in that input-data. Therefore the training and prediction process displayed in Fig. 2.5 was implemented in the model. 70% of the data acquired in the validation study described in section 2.2.1 was used to train the deep learning model, after Post-processing the data. The remaining 30% of the data was then used as test data for the prediction process. This 70/30 split-ratio between training- and test data has been proven as a good approach in previous research [5].

The activity predictions made by the model on the test data were then compared to the actual performed activities. The actual performed activities were at all times known, as during one recording session, repetitions of only one of the defined physical activities were performed. Additionally, the acquired video material was used in order to exactly know which activity was performed when. It shall be once again mentioned that regarding the lifting activities, the lifting and lowering part of the activity were defined as a single activity. This was done for reasons of simplicity because otherwise the model would have become very complex which was not the

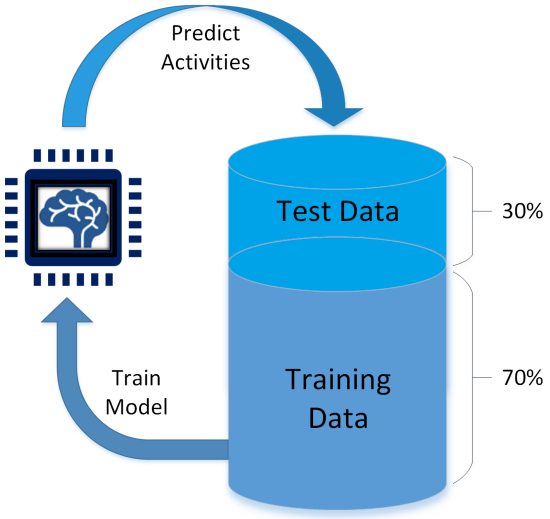

Figure 2.5: 70% of the acquired joint angle data was used to train the deep learning model. The model then predicted activities in the remaining 30% of the data.

intended purpose at this stage of the project.

2.3 Additional features

This section lists additional technology which can be used either in combination with SpineTrack or can use the data provided by SpineTrack and the activity predictions, in order to expand the previously described system. These features can be seen as Add-ons to the SpineTrack system and are only briefly described as they are not the core of this thesis.

The possibility of acquiring data on spinal load moment was explored by using pressure sensing insoles in combination with the SpineTrack system.

Additionally, the activity predictions made by the deep learning model were summarized in a Python-based (Python Software Foundation, Beaverton, OR, USA) web dashboard, which allowed various risk calculations as well as return to work reports.

2.3.1 Load moment estimation

Like previously mentioned, the load moment acting on the low back/spine can lead to occupational low back pain, which can be seen as one of the biggest contributors to WMSDs [19, 22]. Therefore, efforts were taken to combine the SpineTrack system with technology which would allow the estimation of the loads handled by a user, as well as the spinal load moment acting on the user.

Fig. 2.6 displays all the relevant distances in combination with the forces when talking about the load moment acting on the spine, specifically on L5S1. By knowing the height of the person, anthropometric tables [7, 31] can be used to determine all

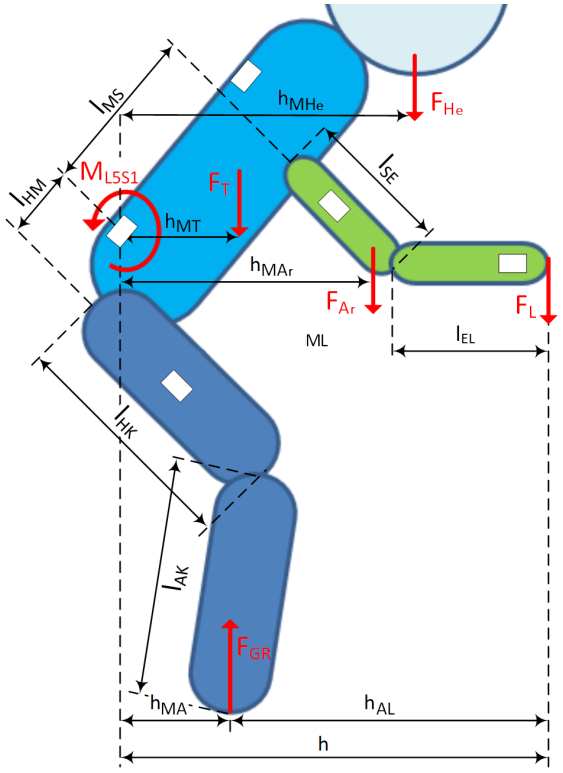

Figure 2.6: Relevant distances, forces and torques for determining the spinal load moment. Distances and forces are defined with the following locations: A=ankle, Ar=Arm, E=elbow, H=hip, He=Head, K=knee, L=load, M=moment, S=shoulder, T=Trunk. Ground reaction force F_{GR}, force acting on the hands while holding a weight F_{L} and spinal load moment of interest acting on L5S1 M_{L5S1}.

the distances except h_{MHe}, h_{MT}, h_{MAr}, h_{MA}, h_{AL} and subsequently h. However, by combining the already determined distances with the obtained joint angles from chapter 2.2.3 and the locations of the centers of mass from Table 2.2, applying simple trigonometry would lead to the latter unknown distances.

Because this was only a pilot experiment, some simplifications have been made in order to determine the load moment, meaning not every distance displayed in Fig. 2.6 was considered.

Fig. 2.7 displays how the horizontal distance h between the weight held in the hands and L5S1 has been calculated. First, the absolute orientation of the IMUs have been used in order determine the orientation of the body segments. From this absolute 3D-orientation only the pitch-angles which differ from the horizontal plane (displayed as θ) have been used. Fig. 2.7(a) displays the unknown horizontal distances related to the upper extremities in red. Fig. 2.7(b) displays the unknown horizontal distance related to the spine. These and the other horizontal distances related to the centers of mass were once again computed using the height of the subject in combination with anthropometric tables [7, 31]. In this computation the assumption is made that the back is straight during the movements, meaning the IMUs T3T4 and L5S1 have the same orientation. Furthermore, it is assumed that

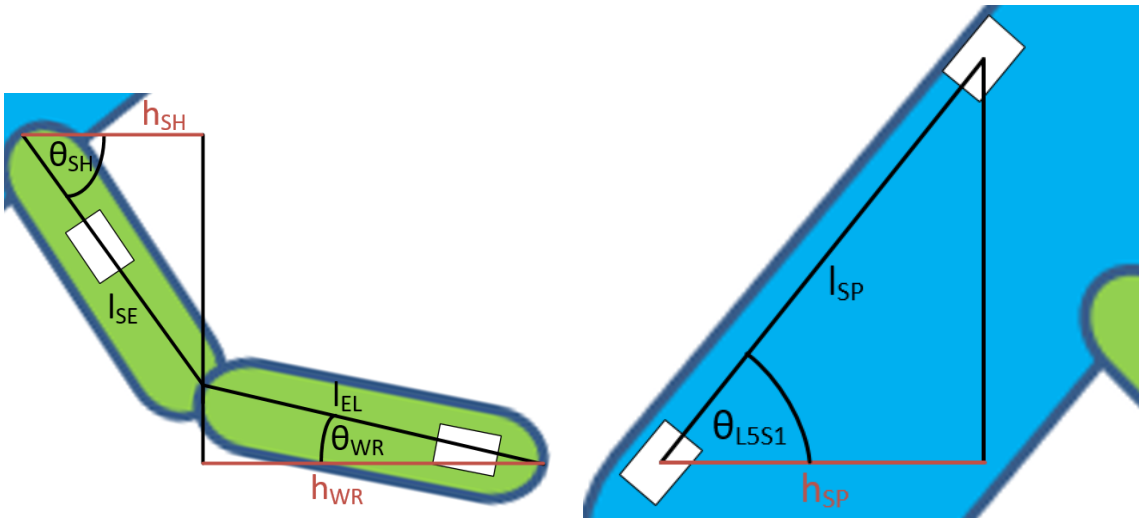

(a) Horizontal distances h_{SH} and h_{WR} related to the upper extremities.

(b) Horizontal distance h_{SP} related to the spine.

Figure 2.7: The horizontal distances which make up the distance h. h is defined as the horizontal distance between the weight held in the hands and L5S1. The known variables are displayed in black while the unknown variables are displayed in red.

the most proximal part of the upper arm overlaps with T3T4 when viewing the sagittal plane, meaning $l_{\mathrm{SP}} \approx l_{\mathrm{MS}}$.

Using the following equations in combination with the segment lengths from Table 2.2, the horizontal distance h was then calculated.

$$h_{\mathrm{WR}} = l_{\mathrm{EL}} \cdot cos(\theta_{\mathrm{WR}}) \tag{2.3}$$

$$h_{\mathrm{SH}} = l_{\mathrm{SE}} \cdot cos(\theta_{\mathrm{SH}}) \tag{2.4}$$

$$h_{\mathrm{SP}} = l_{\mathrm{SP}} \cdot cos(\theta_{\mathrm{L5S1}}) \tag{2.5}$$

$$h = h_{\mathrm{WR}} + h_{\mathrm{SH}} + h_{\mathrm{SP}} \tag{2.6}$$

Using Eq. (2.3) to (2.6) in combination with the locations of the segments specific centers of mass and the corresponding segment weights (gathered from Table 2.2) would be enough information to compute all the moments acting on the spine, generated by the body segment weights. The specific horizontal distances related to the forces F_T, F_{Ar} (consists of the force generated by the upper arm as well as the forearm and the hand) and F_{He} were computed using the same trigonometric procedure previously used.

However, the more interesting aspect of this load moment estimation is the information on the loads being handled by the user. As the purpose of the SpineTrack system is a mobile assessment of the physical demands of a job, therefore also the force measurements should be mobile. Because of this, to obtain information on

Table 2.2: Anthropometric distances and weights relative to subject height H and weight M necessary in order to determine the specific horizontal distances. The location of the centers of mass is determined from proximal. Table adapted from Fig. 4.1 and Table 4.1 from [31]

Body Segment	Segment Length / Body Height	Segment Weight / Body Weight	Location of COM / Segment Length
Head & Neck	0.182H	0.081M	0.5
Upper Arm	0.188H	0.028M	0.436
Forearm & Hand	0.253H	0.022M	0.682
Trunk	0.288H	0.497M	0.5

(a) The transmitter module is strapped to the distal part of the lower leg and connected to the insole via a clip.

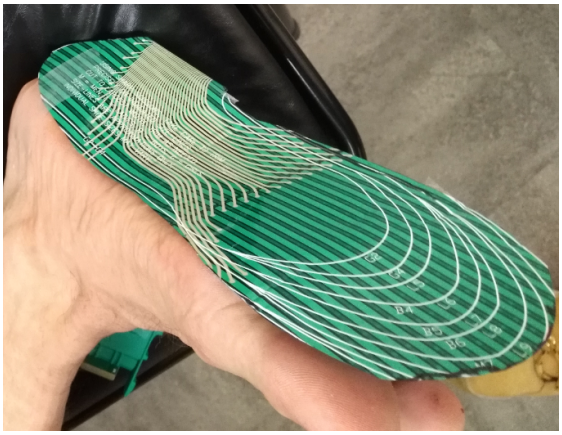

(b) The size of the insole is customized for each subject in order to allow optimal pressure acquisition.

Figure 2.8: Pressure sensing insole applied to a foot using tape as well as a strap to secure the transmitter module.

the ground reaction force F_{GR} and furthermore the loads handled characterized by F_L, pressure sensing insoles (F-Scan, Tekscan Inc., South Boston, MA, USA) were used which output one cumulative force value as well as the location of the center of pressure for each sole. These values were sampled at 100 Hz and stored in .csv-files.

Fig. 2.8 (a) and (b) display these pressure sensing insoles and how they were applied to the foot. First the insoles had to be cut to the shoe size of the subject in order to later on fit in the shoes. Next they were secured to the foot-soles of the subject by means of tape. It was crucial that they were applied in a secure way, otherwise wrinkles could have formed which would lead to loss of pressure data. The pressure-sensitive insoles were then connected to transmitter modules across the lateral sides of the feet. These transmitter modules include various amplifiers and filters which process the raw data in order to be able to transmit it to the PC. The transmitter modules were fixed above the ankles of the subject using straps and were connected to the PC using Ethernet-cables.

The insoles were then calibrated for each subject by following the steps in the provided research software (Tekscan Inc.). Therefore the subjects had to stand on

one leg for five seconds, followed by switching to the other leg and repeating the five seconds stance.

By knowing the users weight before the measurement, it was possible to get information on the load handled F_L when using the pressure sensing insoles. As the forces and distances related to the body segments are known (Trunk: h_{MT}, F_T; Arms: h_{MAr}, F_{Ar}; Head: h_{MHe}, F_{He}), using anthropometric tables, more trigonometric calculations and the previously calculated horizontal distance h, it was possible to calculate the load moment acting on the spine using Eq. (2.7).

$$M_{\mathrm{L5S1}} = F_T \cdot h_{\mathrm{MT}} + F_{\mathrm{Ar}} \cdot h_{\mathrm{MAr}} + F_{\mathrm{He}} \cdot h_{\mathrm{MHe}} + F_L \cdot h \tag{2.7}$$

However, at the time of the creation of this thesis, only pilot experiments have been conducted, meaning the actual computation of the spinal load moment was not validated yet.

The pressure insoles were compared to force plates (AMTI Inc., Watertown, MA, USA) and synchronized to the SpineTrack system by defining a movement the subject had to perform at the start of each recording session. Therefore, the subject lifted its heels which generated a change in force on the force plates as well as on the pressure insoles which then was synchronized to the change in linear acceleration measured by the SpineTrack system.

Generally speaking, the force plates were used as a form of validation for the force output of the pressure sensing insoles. By looking at the differences in the generated force output, the quality and suitability of the pressure sensing insoles for the purposes of SpineTrack could be determined.

3 Results

The following chapter describes all the obtained results, starting with the validation of the joint angles computed by SpineTrack, followed by the results of the activity prediction process and last but not least the results of the pilot study regarding the determination of the load moment using pressure sensing insoles in combination with SpineTrack.

3.1 Kinematics

This section compares the kinematics generated by SpineTrack to the output of the golden standard of a marker based motion capture system. The validation of these kinematics is crucial and a requirement in order to obtain good results during the activity prediction process.

As the validation of the kinematics was executed simultaneously with the pilot study regarding the load moment, the data of only one subject could be acquired. However, as the main purpose of the thesis lies on the activity predictions, one subject can be seen as a first step in order to get an overview on the necessary content of upcoming kinematics validation studies.

The data displayed in the figures in this section were obtained on one subject (gender: female, age: 28, weight: 67.6 kg, height: 166 cm) performing the tasks stated below during a 90-seconds recording session:

- Synchronization at $t = 4\,\mathrm{s}$ by lifting heels.
- Shoulder abductions from $t = 5\,\mathrm{s}$ to $t = 18\,\mathrm{s}$.
- Shoulder scaptions from $t = 19\,\mathrm{s}$ to $t = 29\,\mathrm{s}$.
- Shoulder elevations from $t = 30\,\mathrm{s}$ to $t = 39\,\mathrm{s}$.
- Hip flexions from $t = 40\,\mathrm{s}$ to $t = 53\,\mathrm{s}$.
- Walking from $t = 54\,\mathrm{s}$ to $t = 66\,\mathrm{s}$.
- Carrying a 6 lbs kettlebell from $t = 68\,\mathrm{s}$ to $t = 76\,\mathrm{s}$.
- Carrying a 12 lbs kettlebell from $t = 80\,\mathrm{s}$ to $t = 86\,\mathrm{s}$.

Fig. 3.1 displays the spine angle φ_{TR} generated by SpineTrack, computed using the difference quaternion between sensors L5S1 and T3T4, in comparison to the spine angle determined by the motion capture system. The Y-axis of SpineTrack is determined in a way that it lines up with the computed X-axis of the motion

capture system. Fig. 3.1(a) displays the whole 90 seconds of the recording session while Fig. 3.1(b) focuses on the performed hip flexions.

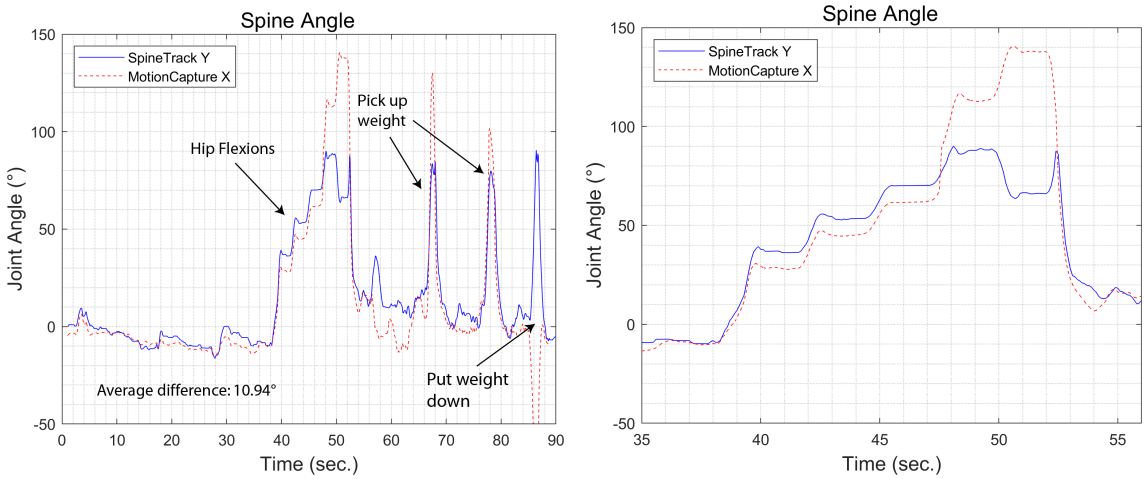

(a) Spine angle with highlighted actions across the whole recording session.

(b) Spine angle during hip flexions from $t = 35\,\mathrm{s}$ to $t = 56\,\mathrm{s}$.

Figure 3.1: Computed spine angle φ_{TR} using the SpineTrack L5S1- and T3T4 sensors in comparison to motion capture output. Various tasks were performed during the recording session which lead to different requirements for the spine angle.

Fig. 3.2(a) and Fig. 3.2(b) display the flexion angles φ_{SF} of the left- and the right shoulder respectively across the whole recording session. The difference quaternions between sensors T3T4 and LSH/RSH were calculated in order to determine these joint angles.

Fig. 3.3(a) and Fig. 3.3(b) display the flexion angles of right- and left elbow joint respectively, by calculating the difference quaternion between sensors LSH/RSH and LWR/RWR.

The last two figures in the kinematic results display the left and right thigh inclinations acquired by SpineTrack. Unfortunately, the motion capture system did not output reliable thigh inclination angles, therefore only the SpineTrack output is displayed in Fig. 3.4(a) and Fig. 3.4(b). Fig. 3.4(b) displays the carrying pattern (6 lbs kettlebell) from $t = 65\,\mathrm{s}$ to $t = 80\,\mathrm{s}$.

3.2 Activity prediction

This section describes the achieved results regarding the activity prediction process using the implemented deep learning model. The predictions are hereby validated by means of a comparison to the actual performed activities.

There were 17 healthy subjects (10 males) in the laboratory validation study with an average age of 31 ± 13.6 years. The average height and weight of individuals were 169.4 ± 14.8 cm and 68.5 ± 15.6 kg, respectively.

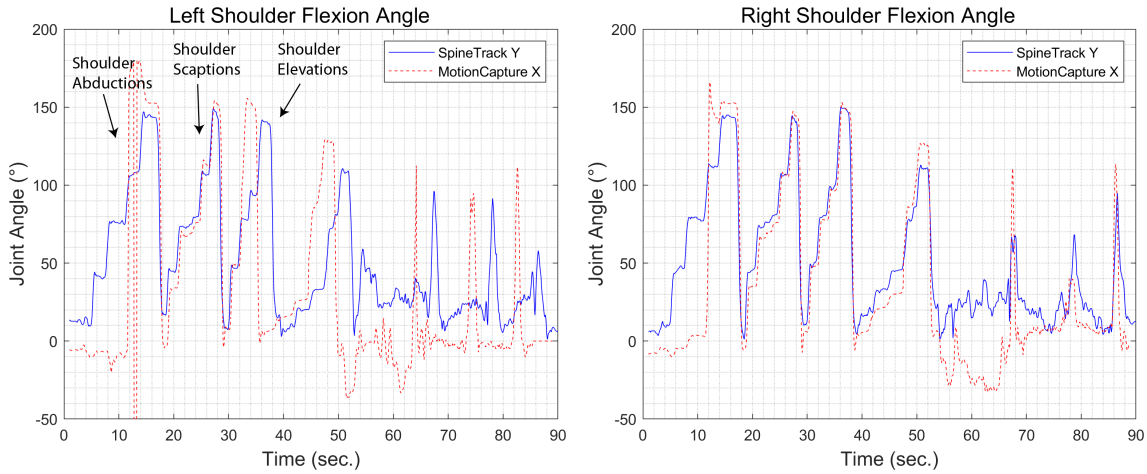

(a) Flexion angle of the left shoulder with highlighted actions across the whole recording session.

(b) Flexion angle of the right shoulder across the whole recording session.

Figure 3.2: Computed flexion angle φ_{SF} of the left- and right shoulder using the SpineTrack T3T4- and LSH/RSH sensors in comparison to motion capture output. Various levels of abductions, scaptions and elevations were performed during the recording session.

Fig. 3.5 displays a subject performing two of the physical activities during the validation study. (a) displays a lift to shoulder level (ID 5) while (b) displays a carrying task (ID 0).

The deep learning model achieved an overall accuracy of 96.66% for predicting activities correctly.

Regarding the usability of the SpineTrack system, the subjects psycho-physical impressions, extracted from surveys, can be summarized as follows: On a scale of 1 to 10, with 1 being the least and 10 being the most, the subjects reported an average fatigue-level of 3.5 ($\pm$2.5) after the completion of the trial. 11 out of the 17 subjects stated that they could imagine themselves wearing the device across a whole workday.

3.3 Load moment

This section describes the results achieved regarding the computation of the load moment acting on the spine. As this part of the project was only an additional feature, there was no major focus on these results.

The load moment acting on the spine could not be fully computed in this thesis due to time constraints. However, the following results are from a pilot study with one subject (gender: female, age: 28, weight: 67.6 kg, height: 166 cm) in order to get an overview on how the load moment could be calculated in the future.

Fig. 3.6 displays this subject performing a task in the form of a weighted hip flexion.

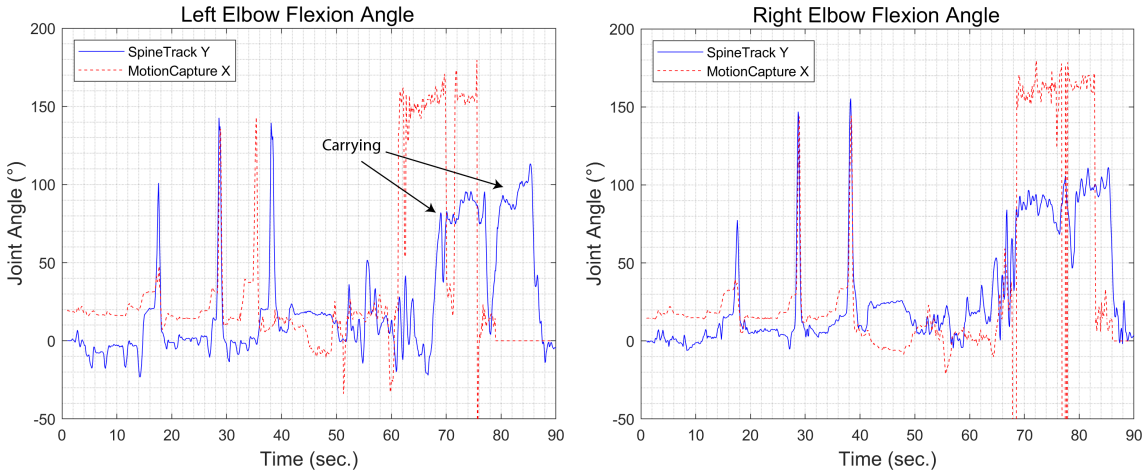

(a) Flexion angle of the left elbow with highlighted actions across the whole recording session.

(b) Flexion angle of the right elbow across the whole recording session.

Figure 3.3: Computed flexion angle φ_{EF} of the left- and right elbow using the SpineTrack LSH/RSH- and LWR/RWR sensors in comparison to motion capture output.

Fig. 3.7 displays the results of this task while wearing the SpineTrack device, pressure sensing insoles and while standing on force plates. The hip flexion angle generated by SpineTrack is displayed as well as the force measured by the pressure sensing insoles and force plates. Additionally the difference in measured force between insoles and force plates is shown as a dashed line.

The subject walked on the force plates from $t = 0\,\mathrm{s}$ to $t = 5\,\mathrm{s}$ and lifted her heels from $t = 5\,\mathrm{s}$ to $t = 7\,\mathrm{s}$ in order to synchronize the systems. From $t = 10\,\mathrm{s}$ to $t = 12\,\mathrm{s}$ the subject picked up a 12 lbs kettlebell and performed weighted hip flexions from $t = 20\,\mathrm{s}$ to $t = 35\,\mathrm{s}$. The subject put the weight back on the ground at $t = 35\,\mathrm{s}$.

The weight of the subject is highlighted at $t = 8\,\mathrm{s}$ as well as the increase in weight when the subject picked up the kettlebell. The average difference in force measured between the force plates and the pressure sensing insoles was 161.72 N (16.49 kg) which translates to an average difference of 24.3% of body weight.

Because of this difference in forces, another recording session consisting of the subject just standing still has been executed. Fig. 3.8 displays this recording, where the subject stepped on the force plate at $t = 1\,\mathrm{s}$ and synchronized the two systems during $t = 4\,\mathrm{s}$ and $t = 7\,\mathrm{s}$. For the rest of the recording session, the subject did not move. The average difference in measured forces was 196.76 N (20.05 kg) which translates to 29.6% of the body weight of the subject.

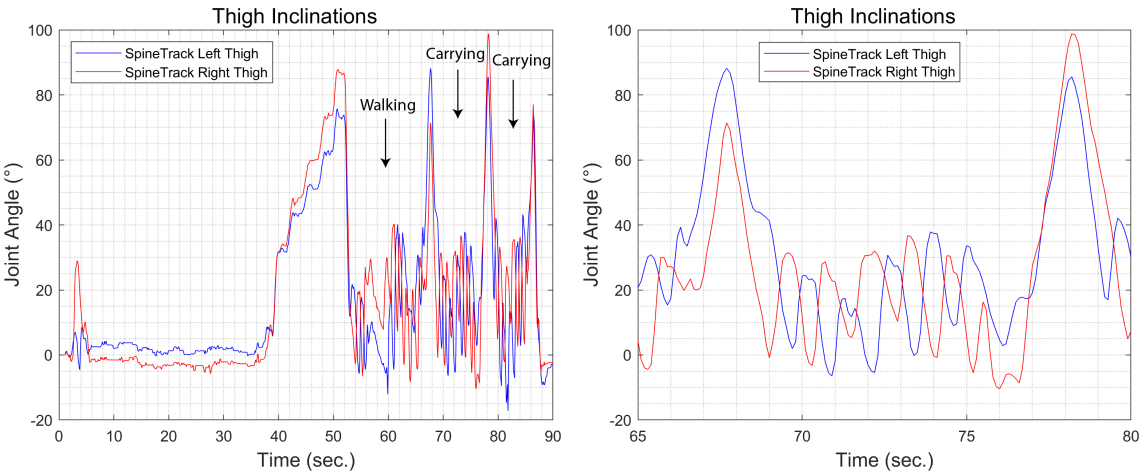

(a) Inclination angle of the left and right thigh with highlighted actions across the whole recording session.

(b) Thigh inclination angles during carrying from $t = 65\,\mathrm{s}$ to $t = 80\,\mathrm{s}$.

Figure 3.4: Computed inclination angle of the left- and right thighs using the SpineTrack L5S1- and LTH/RTH sensors. Various functional tasks were performed to review the performance of the SpineTrack system.

(a) A subject is performing a lift to shoulder height while wearing SpineTrack.

(b) A subject is performing a carrying task while wearing SpineTrack.

Figure 3.5: A subject is performing different physical activities during the validation study while wearing SpineTrack. Subjects were guided through the execution of these tasks. The generated data was then used to train and validate the deep learning model.

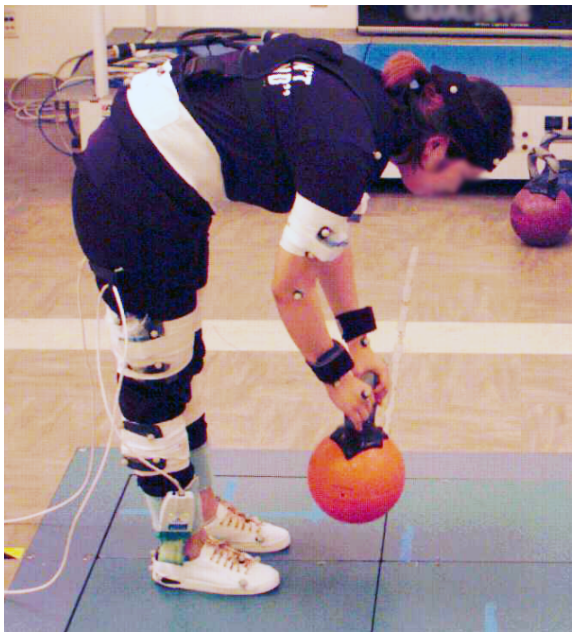

Figure 3.6: A subject is wearing SpineTrack while performing a weighted hip flexion. Additionally the kinematics of the subjects are tracked via markers using a motion capture system. The subject is performing the movement while wearing pressure sensing insoles and while standing on a force plate.

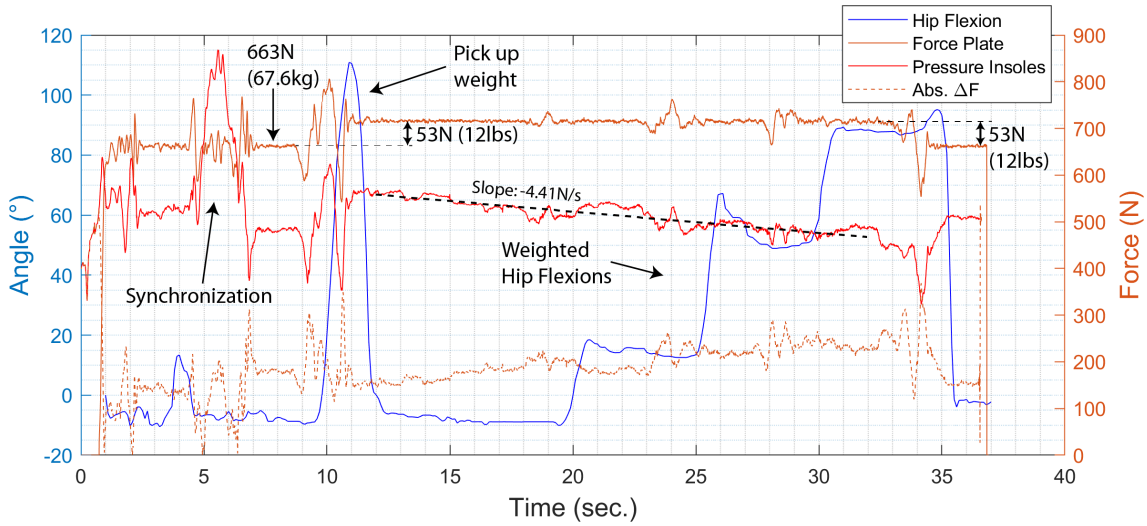

Figure 3.7: Computed hip flexion angle φ_{HF} using the SpineTrack L5S1- and RTH sensors. Ground reaction forces were acquired using force plates as well as pressure sensing insoles. The absolute difference in the acquired forces is displayed as a dashed brown line. Specific actions and weights are highlighted.

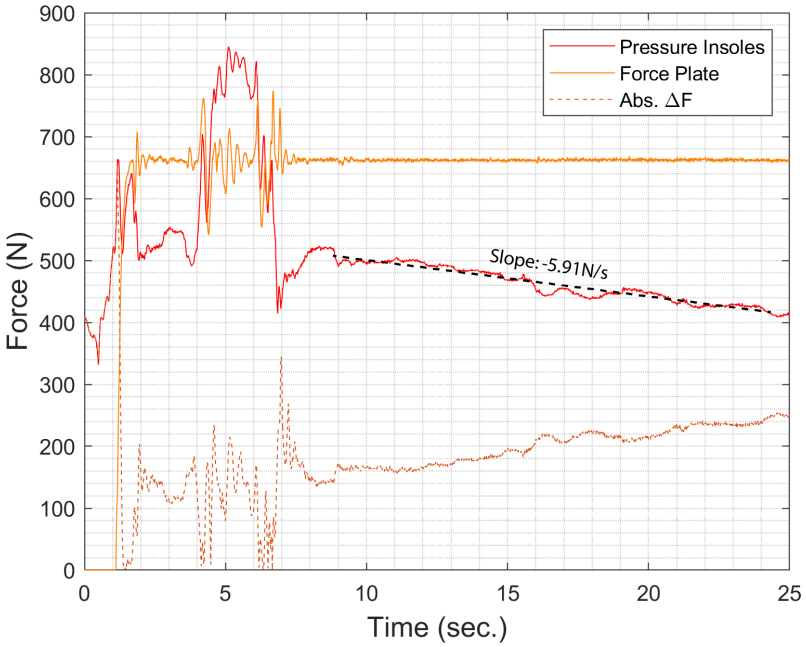

Figure 3.8: Ground reaction forces during the static task of standing. These values were acquired using force plates as well as pressure sensing insoles. The absolute difference in the acquired forces is displayed as a dashed brown line.

4 Discussion and Outlook

The following chapter reflects and interprets all the obtained results in a critical way. First the achieved kinematics with SpineTrack are discussed, followed by the deep learning model and the results regarding the load moment estimation. In the end, an outlook on future work is given.

4.1 Kinematics

This section discusses the comparison of the kinematics acquired with SpineTrack and the motion capture system.

The kinematics of the spine angle φ_{TR} generated by SpineTrack and the motion capture system, depicted in Fig. 3.1, generally align quite well. However, when looking at the actual values of the magnitudes, some differences are visible. The hip flexions from $t = 40\,\mathrm{s}$ to $t = 53\,\mathrm{s}$ have the same shapes except the last part, where the spine angle generated by SpineTrack suddenly heads in the opposite direction. This can be seen as an artifact, as the angle should increase instead of decrease. It could be caused by an unintentional shifting of an IMU. The increase in φ_{TR}, when the subject is picking up weights aligns, however the absolute values are different from each other. This could be caused by the fact that there is an on-board low pass filter in the IMUs which removes high frequency noises. This unfortunately also suppresses rapid changes in the joint angles, which could explain the attenuated peaks. The inverted peak of the motion capture data at $t = 86\,\mathrm{s}$ is definitely an artifact and could be caused by obstructed markers during the recording session. It shall be mentioned here, that the problem with obstructed markers and subsequently bad motion capture joint angle data seems to be a problem with the marker model displayed in Appendix A. The average joint angle difference with $10.94\,^\circ$ seems rather big, however this value includes all the mentioned artifacts. The computation of the spine angle by SpineTrack can be seen as sufficiently accurate for the deep learning model.

The kinematics of the left shoulder flexion angle φ_{SF} depicted in Fig. 3.2(a) are a bit harder to interpret as the motion capture data once again seems to be a bit unreliable. There is some motion capture data missing, hence a temporal shift starting at the shoulder elevations. However, the general shape of the curves seem to align well. The average difference in joint angle is not depicted as the temporal offset would lead to unrealistically high differences.

The kinematics of the right shoulder flexion angle depicted in Fig. 3.2(b) align extremely well most of the time, however once again the motion capture data shows artifacts which lead to differences in joint angle data. During the scaption and

elevation movements the average difference in joint angle is below 5 ° which can be seen as a very satisfying result.

Once again, unreliable motion capture joint angle data is visible in Fig. 3.3(a) and 3.3(b). The overall shapes of these left- and right elbow flexion angles φ_{EF} do align, however further analysis of this comparison can not be made, as the motion capture data includes too many artifacts. The SpineTrack data once again seems to be more realistic as all of the peaks displayed in the graphs actually make sense when looking at which movement was performed each time. For example, when looking at the carrying-movement at the end of the recording session, an elbow flexion angle of around 90 ° is constantly visible, which is in fact necessary to carry an object at waist level when using both hands.

The thigh inclination angles displayed in Fig. 3.4 are solely generated by SpineTrack, as the motion capture kinematic data for the lower extremities unfortunately could not be used because of too many artifacts and general inconsistencies. These angles could also be described as hip flexions, as the difference in orientation between the L5S1- and the thigh-sensors are plotted here. These results seem very reliable because the angles do not change during the static positions in the beginning of the recording session and the hip flexions can be clearly seen starting at $t = 40\,\mathrm{s}$. Also the kinematic pattern during walking and carrying seems very plausible as the joint angles increase and decrease periodically and inversely when comparing the left and right thigh inclinations as displayed in Fig. 3.4(b).

Overall, the kinematic results generated by SpineTrack can be seen as very reliable and therefore should be more than suitable as input data for the deep learning model. However, it is a bit unfortunate that no complete validation of the kinematics could be performed because of the artifacts in the motion capture data.

4.2 Activity prediction

This section discusses the results achieved in the prediction process using the deep learning model which is the main focus of this thesis.

The actual summary table of the prediction results could not be displayed in this thesis due to reasons of intellectual property. The achieved overall accuracy of 96.6% for the 4765 predictions seems like an extremely high value, given the rather small amount of only 17 subjects. However, one has to be careful when interpreting this data. As Fig. 2.5 displays, the test data which includes the 4765 executed activities, was taken from the same dataset in which the training data was included. Therefore a high overall accuracy was to be expected from the beginning. A better test for the deep learning model would be to use data which includes actual occupational tasks as input (drilling, painting, cleaning etc.) and observe if the deep learning model is able to extract the defined 23 physical activities (see Table 2.1) out of this data. Tests were already made using some of these occupational tasks in combination with a three seconds classification window and the model achieved an accuracy level of around 85% this way. This accuracy level can be still seen as quite good, however it would increase even further with an increased sample size (e.g. from 17 subjects to 30 subjects).

Generally speaking, a trend of misclassifications is visible from activity 4 to activity 11. These activities are all defined as lifting activities when looking at Table 2.1. Because of their similarity, misclassifications were bound to happen in these activities. The goal therefore is to keep these wrong classifications relatively low and to not let them get out of hand. This could be achieved by the previously mentioned increase in sample size, which would allow a more intensive training of the model. Another way of increasing the accuracy of the model would be the gathering of additional information, next to acquiring the joint angle data. The estimation of the load moment during a lift using pressure sensing insoles, would for example drastically improve the accuracy of the model, especially for the prediction of lifting activities.

However, when comparing the actual number of correctly classified activities to the wrongly classified ones, it is visible that the correct classifications outweigh the misclassifications by factors 20 and upwards. Therefore, the overall accuracy of the model can be seen as very satisfying at this stage of development.

The experimental protocol in itself can be also seen as successful, as a lot of data was collected from each subject, while not fatiguing them too much. A low fatigue-level generally leads to better data, as subjects tend to change their movements with increased fatigue.

4.3 Load moment

This section describes and discusses the acquired data regarding the load moment estimation using SpineTrack when comparing pressure sensing insoles to force plates.

Fig. 3.7 shows the results of the first attempt on combining the SpineTrack system with force data while performing tasks. The synchronization from $t = 5\,\mathrm{s}$ to $t = 7\,\mathrm{s}$ is easily visible in the force plate- as well as in the pressure insoles data. However, it was a bit tricky to synchronize the kinematics generated by SpineTrack to the force data. The synchronization movement of lifting the heels could only be seen slightly in the generated acceleration data which makes exact synchronization difficult. A different movement which influences the force data as well as the kinematic data by affecting the orientation of one of the IMUs (e.g. lifting up one thigh) may be more suitable in this case.

It can be clearly seen when the subjects bends down to pick up the 12 lbs weight at $t = 10\,\mathrm{s}$ by observing the hip flexion. A hip flexion angle of around 110° while picking up an object can generally be seen as realistic. The kinematic data during the subsequent hip flexions also looks very realistic as three levels of increasing hip flexions were performed. All in all, the kinematic data appears to be once again very reliable.

There seems to be a prominent difference between the force values from the force plate and from the pressure sensing insoles. However, the correct force values can certainly be obtained from the force plate data, as the force value of 663 N at $t = 7\,\mathrm{s}$ directly translates to the previously obtained body weight of the subject (67.6 kg). In comparison, when looking at the data obtained by the pressure sensing insoles, a force value of 482 N can be observed, which would lead to a body weight of 49.13 kg.

This 27.4% difference in measured force is very problematic, as in order to sufficiently estimate the load moment acting on the spine, it is crucial that the ground reaction force (see Fig. 2.6) is known with a certain degree of accuracy.

After the subject picked up the 12 lbs kettlebell at $t = 10\,\text{s}$, a 53 N increase of the force can be seen at the force plate which exactly translates to the weight of the kettlebell. However, in the case of the pressure sensing insoles, an increase of 83.2 N is observed this time, which would translate to a 18.7 lbs kettlebell instead of a 12 lbs one.

If this difference between the force plate and the pressure sensing insoles would be constant, it would be easy to compensate for, by introducing correction factors. When comparing the force values from $t = 20\,\text{s}$ to $t = 35\,\text{s}$ during the hip flexions, it is visible that the data acquired by the pressure sensing insoles indeed starts to drift downwards continuously. The curve thereby decreases by 4.41 N per second. One could think this drift could be caused by the change of the center of pressure during the hip flexions.

When observing Fig. 3.8, it becomes clear that this drift is in fact not caused by the shift of the center of pressure, as during this task the subject was standing still with no movement at all. In this case the curve drifts downwards even faster with a value of 5.91 N per second.

When looking at the dashed lines of both figures, which indicate the absolute differences in force values, a nonlinear trend can be observed. This nonlinear trend does not allow a proper estimation of the ground reaction force, it would only be possible to compensate for the drift when the subject is standing still. However, when using SpineTrack, dynamic changes of the ground reaction force are also of interest. Therefore it was decided that this type of pressure insole is not suitable for the purpose of SpineTrack.

For reasons of time, the actual computation of the load moment acting on the spine could not be performed in this thesis.

4.4 Conclusion and outlook

This section aims to reflect on the SpineTrack-advancements presented in this thesis and provides an outlook on future work necessary in order to be able to successfully use the device on the job-site.

The kinematics generated by SpineTrack generally allow a proper tracking of body-segment orientation. However, the presented validation of the kinematics can not be seen as satisfying yet. The validation was performed using only one subject and some of the motion capture data, used to validate the kinematics, seemed unreliable. Therefore, as a next step, a complete validation study, including at least twelve subjects shall be performed. This would allow a comprehensive analysis of the kinematics supplied by SpineTrack, which could then be used to further improve the tracking of the body-segment orientations.

The advancements with the deep learning model can be seen as very successful. However, this was just the first step of the development of the model, as a next step the model shall be applied to functional task data, meaning data which is comprised

of different physical activities and which is not included in the training data. This functional task data would then provide an actual overview on the quality of the current state of the model.

Getting information on the loads handled as well as the load moment acting on the spine can be seen as extremely crucial. Having this information available during a physical activity would allow the deep learning model to classify activities with accuracy levels way above the previously achieved ones. It would also provide very valuable information on the risk for development of WMSDs, as it is the number one cause of these diseases. Therefore, acquiring the load moment shall be seen as a priority in the further development of SpineTrack. Different pressure sensing insoles shall be used in the future, which allow a more precise determination of the ground reaction force, also during dynamic tasks.

This thesis presented the current state and ongoing advancements of SpineTrack. SpineTrack has the potential to substantially contribute to the decrease of WMSDs by summarizing the physical demands and risk factors of different job sectors. Future work is still necessary, however the current progress in developments seems very promising.

Bibliography

[1] Blanco, J.L., 2013. A tutorial on SE(3) transformation parameterizations and on-manifold optimization. University of Malaga.

[2] CCOHS, 2013. Osh answers fact sheets: Mmh - introduction. URL: `https://www.ccohs.ca/oshanswers/ergonomics/mmh/mmhintro.html`.

[3] Center for Disease Control and Prevention, 2012. National health interview survey. URL: `https://www.cdc.gov/nchs/nhis/nhis_2012_data_release.htm`.

[4] Coenen, P., Kingma, I., Boot, C.R.L., Twisk, J.W.R., Bongers, P.M., van Dieën, J.H., 2013. Cumulative low back load at work as a risk factor of low back pain: a prospective cohort study. Journal of occupational rehabilitation 23, 11–18.

[5] Crowther, P.S., Cox, R.J., 2005. A method for optimal division of data sets for use in neural networks, in: Hutchison, D., Kanade, T., Kittler, J., Kleinberg, J.M., Mattern, F., Mitchell, J.C., Naor, M., Nierstrasz, O., Pandu Rangan, C., Steffen, B., Sudan, M., Terzopoulos, D., Tygar, D., Vardi, M.Y., Weikum, G., Khosla, R., Howlett, R.J., Jain, L.C. (Eds.), Knowledge-Based Intelligent Information and Engineering Systems. Springer Berlin Heidelberg, Berlin, Heidelberg. volume 3684 of *Lecture Notes in Computer Science*, pp. 1–7.

[6] Gauthier, F., Gelinas, D., Marcotte, P., 7/24/2010 - 7/27/2010. Vibration of portable orbital sanders and its impact on the development of work-related musculoskeletal disorders in the furniture industry, in: The 40th International Conference on Computers & Indutrial Engineering, IEEE. pp. 1–5.

[7] Gordon, C.C., Blackwell, C.L., Bradtmiller, B., Parham, J.L., Barrientos, P., Paquette, S.P., Corner, B.D., Carson, J.M., Venezia, J.C., Rockwell, B.M., Mucher, M., Kristensen, S., 2014. 2012 Anthropometric Survey of U.S. Army Personel: Methods and Summary Statistics. U.S. Army Natick Soldier Research, Development and Engineering Center.

[8] Hanson, A., 2006. Visualizing quaternions. The Morgan Kaufmann series in interactive 3D technology, Morgan Kaufmann, San Francisco, Calif. and London.

[9] Haslwanter, T., 2018. 3D Kinematics. Springer International Publishing.

[10] Health and Safety Executive, 2005. Hand-arm vibration exposure calculator. URL: `http://www.hse.gov.uk/vibration/hav/vibrationcalc.htm`.

[11] Hignett, S., McAtamney, L., 2000. Rapid entire body assessment (reba). Applied ergonomics 31, 201–205.

[12] Hochreiter, S., Schmidhuber, J., 1997. Long short-term memory. Neural Computation 9, 1735–1780.

[13] Liberty Mutual Insurance, 2004. Manual materials handling guidelines: Tables for evaluating lifting, lowering, pushing, pulling and carrying tasks .

[14] Liberty Mutual Insurance, 2018. Liberty mutual workplace safety index. URL: https://business.libertymutualgroup.com/business-insurance/Documents/Services/Workplace%20Safety%20Index.pdf.

[15] Marras, W.S., 2000. Occupational low back disorder causation and control. Ergonomics 43, 880–902.

[16] Marras, W.S., Lavender, S.A., Leurgans, S.E., Rajulu, S.L., Allread, W.G., Fathallah, F.A., Ferguson, S.A., 1993. The role of dynamic three-dimensional trunk motion in occupationally-related low back disorders. the effects of workplace factors, trunk position, and trunk motion characteristics on risk of injury. Spine 18, 617–628.

[17] McAtamney, L., Nigel Corlett, E., 1993. Rula: a survey method for the investigation of work-related upper limb disorders. Applied ergonomics 24, 91–99.

[18] McGill, S.M., 1997. The biomechanics of low back injury: Implications on current practice in industry and the clinic. Journal of Biomechanics 30, 465–475.

[19] McGill, S.M., Hughson, R.L., Parks, K., 2000. Changes in lumbar lordosis modify the role of the extensor muscles. Clinical Biomechanics 15, 777–780.

[20] Merryweather, A.S., Loertscher, M.C., Bloswick, D.S., 2009. A revised back compressive force estimation model for ergonomic evaluation of lifting tasks. Work (Reading, Mass.) 34, 263–272.

[21] National Institute for Occupational Safety and Health, 1997. Musculoskeletal disorders and workplace factors: a critical review of epidemiologic evidence for WMSDs of the neck, upper extremity and low back. US Department of Health and Human Services, Center for Diseases Control and Prevention, NIOSH.

[22] Pope, M.H., Goh, K.L., Magnusson, M.L., 2002. Spine ergonomics. Annual review of biomedical engineering 4, 49–68.

[23] Punnett, L., Prüss-Utün, A., Nelson, D.I., Fingerhut, M.A., Leigh, J., Tak, S., Phillips, S., 2005. Estimating the global burden of low back pain attributable to combined occupational exposures. American journal of industrial medicine 48, 459–469.

[24] Safety and Health Assessment and Research for Prevention Program, 2004. Injured at Work: What workers' compensation data reveal about work-related musculoskeletal disorders. Summary of Technical Report Number 40-8a-2004.

[25] Shackel, B., 1974 (1982). Applied ergonomics handbook. Butterworth, London.

[26] Simoneau, S., St-Vincent, M., Chicoine, D., 1996. Work-related Musculoskeletal Disorders (WMSDs): A better understanding for more effective prevention. Institut de recherche Robert-Sauve en sante et en securite du travail du Quebec.

[27] Stack, T., Ostrom, L.T., Wilhelmsen, C.A., 2016. Occupational ergonomics: A practical approach / Theresa Stack, Lee T. Ostrom, Cheryl A. Wilhelmsen. 1st ed., John Wiley & Sons, Hoboken, New Jersey.

[28] The-Mathworks-Inc., 2019. plotconfusion() documentation. URL: `https://de.mathworks.com/help/deeplearning/ref/plotconfusion.html`.

[29] United States Bone and Joint Initiative, 2014. The Burden of Musculoskeletal Diseases in the United States: Prevalence, Societal and Economic Cost. 3 ed.

[30] Waters, T.R., Vern, P.A., Arun, G., 1994. Applications Manual for the Revised NIOSH Lifting Equation. National Institute for Occupational Safety and Health.

[31] Winter, D.A., 2009. Biomechanics and motor control of human movement. 4th ed. ed., Wiley and Chichester : John Wiley [distributor], Hoboken, N.J.

[32] Woodman, O.J., 2007. An introduction to inertial navigation. University of Cambridge.

Appendix A

SMU Cluster Marker Set for Manual Materials Handling (MMH) Research — *April 2019*

STATIC MARKERS ○	DIAGRAMS	● DYNAMIC MARKERS
Pelvis 1. RASI 2. LASI *Right Thigh* 3. RFLE 4. RFME *Right Lower Leg* 5. RLMA 6. RMMA *Left Thigh* 7. LFLE 8. LFME *Left Lower Leg* 9. LLMA 10. LMMA *(Remove markers after STATIC trial)*	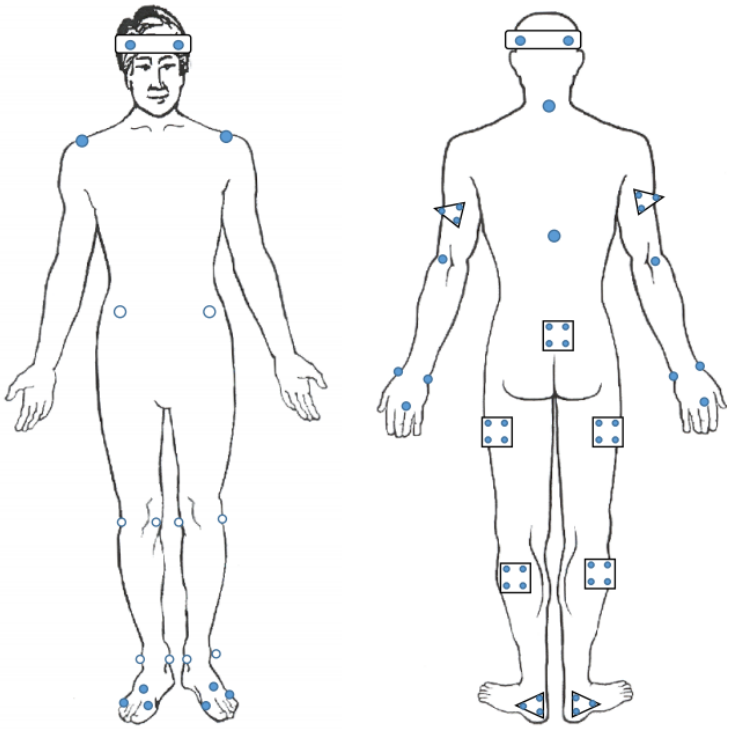	*Single Markers* *Trunk* 1. RACR 2. LACR 3. CER7 4. TH10 *Right Arm* 5. RELB 6. RULN 7. RRAD 8. RMCP *Left Arm* 9. LELB 10. LULN 11. LRAD 12. LMCP *Right Foot* 13. R1MT 14. R3MT 15. R5MT *Left Foot* 16. L1MT 17. L3MT 18. L5MT *Cluster Markers* 1. RFHD, LFHD, RRHD, LRHD 2. RARM, RAMS, RAMI 3. LARM, LAMS, LAMI 4. LPSI, RPSI, RPII, LPII 5. RTH1, RTH2, RTH3, RTH4 6. RSH1, RSH2, RSH3, RSH4 7. RSCA, RICA, RLCA 8. LTH1, LTH2, TTH3, LTH4 9. LSH1, LSH2, LSH3, LSH4 10. LSCA, LICA, LLCA

Marker positions used in the motion capture system in order to generate a full kinematic model of the subject. Static markers, depicted as empty circles, were removed after the calibration procedure. The markers were attached using tape and straps in order to prevent any displacement during the trial.